

The Cushion Region and Dayside Magnetodisc Structure at Saturn

Ned Russell Staniland¹, Michele K. Dougherty², Adam Masters¹, and Nicholas Achilleos³

¹Imperial College London

²Imperial College

³University College London

November 28, 2022

Abstract

A sustained dipolar magnetic field between the current sheet outer edge and the magnetopause, known as a cushion region, has yet to be observed at Saturn. Whilst some signatures of reconnection occurring in the dayside magnetodisc have been identified, the presence of this large-scale structure has not been seen. Using the complete Cassini magnetometer data, the first evidence of a cushion region forming at Saturn is shown. Only five potential examples of a sustained cushion are found, revealing this phenomenon to be rare. This feature more commonly occurs at dusk compared to dawn, where it is found at Jupiter. It is suggested that due to greater heating and expansion of the field through the afternoon sector the disc is more unstable in this region. We show that magnetodisc breakdown is more likely to occur within the magnetosphere of Jupiter compared to Saturn.

The Cushion Region and Dayside Magnetodisc Structure at Saturn

N. R. Staniland¹, M. K. Dougherty¹, A. Masters¹, and N. Achilleos²

¹Blackett Laboratory, Imperial College London, London, UK

²Department of Physics and Astronomy, University College London, Gower St., London WC1E 6BT

Key Points:

- The first example of a cushion region at Saturn is identified at dusk
- The dawn magnetodisc structure is less likely to break down close to the magnetopause compared to dusk
- Jupiter is more likely to have a cushion region compared to Saturn primarily due to system size

Corresponding author: Ned Russell Staniland, n.staniland17@imperial.ac.uk

12 **Abstract**

13 A sustained dipolar magnetic field between the current sheet outer edge and the
 14 magnetopause, known as a cushion region, has yet to be observed at Saturn. Whilst some
 15 signatures of reconnection occurring in the dayside magnetodisc have been identified, the
 16 presence of this large-scale structure has not been seen. Using the complete Cassini mag-
 17 netometer data, the first evidence of a cushion region forming at Saturn is shown. Only
 18 five potential examples of a sustained cushion are found, revealing this phenomenon to
 19 be rare. This feature more commonly occurs at dusk compared to dawn, where it is found
 20 at Jupiter. It is suggested that due to greater heating and expansion of the field through
 21 the afternoon sector the disc is more unstable in this region. We show that magnetodisc
 22 breakdown is more likely to occur within the magnetosphere of Jupiter compared to Sat-
 23 urn.

24 **Plain Language Summary**

25 **1 Introduction**

26 At the gas giants, the presence of an internal plasma source coupled with their rapid
 27 rotation (approximately 10 hours) significantly perturbs their magnetic field configura-
 28 tion. Mass ejected from the moons Enceladus and Io in the inner magnetosphere of Sat-
 29 urn and Jupiter, respectively, becomes ionised, locking onto magnetic field lines and is
 30 accelerated towards corotation. The newly-formed plasma is centrifugally confined to the
 31 equator, radially stretching the magnetic field into a magnetodisc. This structure has
 32 been observed at all local times under expanded conditions at Saturn (Arridge, Russell,
 33 et al., 2008). At Jupiter, a region adjacent to the magnetopause where the magnetodisc
 34 structure breaks down and the field is dipolar, referred to as the “cushion region”, has
 35 been identified (Went, Kivelson, et al., 2011) and is argued to be populated by mass-depleted
 36 flux tubes following tail reconnection (Kivelson & Southwood, 2005). However, this re-
 37 gion has yet to be identified at Saturn (Went, Kivelson, et al., 2011), despite the sim-
 38 ilarities between these two systems.

39 At Saturn, mass that is loaded into the magnetosphere by Enceladus must be lost
 40 from the system. These water group ions, written as W^+ , are eventually driven radially
 41 outwards in the low plasma beta ($\beta < 1$) inner magnetosphere via an interchange in-
 42 stability with the more tenuous hot plasma population in the outer magnetosphere (Gold,
 43 1959). At larger radial distances, plasma pressure dominates ($\beta > 1$) and the magnetic
 44 field balloons until closed field lines reconnect and mass is lost in the magnetotail (Vasyliunas,
 45 1983). Hence, mass-depleted flux tubes following nightside reconnection via this cycle,
 46 or the solar-wind driven Dungey cycle (Dungey, 1961), convect along the dawn flanks
 47 towards noon and are subsequently refilled, thus restarting the mass transport cycle. It
 48 has been suggested that a turbulent channel of mass-depleted flux tubes should then re-
 49 side radially outwards of the magnetodisc, where the field geometry is dipolar due to the
 50 lower mass content and a breakdown of the disc. This region is regarded as a signature
 51 of these cycles and has been identified at Jupiter (Kivelson & Southwood, 2005; Went,
 52 Kivelson, et al., 2011). However, since the arrival of Juno, Gershman et al. (2018) found
 53 there lacked a systematic cushion region at Jupiter, possibly highlighting that this dy-
 54 namical picture is incomplete.

55 Evidence of supercorotating return flow at dawn following Vasyliunas-type recon-
 56 nection has been identified at Saturn (Masters et al., 2011). Jasinski et al. (2019) iden-
 57 tified a region of mass depleted flux tubes in the morning sector using the data from the
 58 CAPS Electron Spectrometer (ELS) instrument (Young et al., 2004). Yet a dipolar struc-
 59 ture has not been seen in the magnetic field data (Went, Kivelson, et al., 2011). Delamere
 60 et al. (2015) argue that the cushion region is an inevitable consequence of magnetodisc
 61 formation. However, their criteria for identifying a cushion, given by $B_\theta > B_{dipole}$ at

62 the equator, where B_θ is the north-south magnetic field component and B_{dipole} is the
 63 dipole field strength, does not capture the structure described above. It does not con-
 64 sider that the current sheet magnetic field reverses sign from northward to southward
 65 towards its outer edge. This adds to the total magnetic field and therefore fulfils their
 66 criteria without that region necessarily containing expelled content from the current sheet.
 67 To identify whether the cushion is sustained over large scales, an analysis of how the global
 68 magnetic field structure varies with distance from the planet is required.

69 This study will use the complete Cassini orbital magnetometer dataset at Saturn
 70 (Dougherty et al., 2004) to show the first evidence of a cushion region at Saturn. This
 71 region is found to arise preferentially at dusk, rather than dawn as was previously ex-
 72 pected. We suggest this is due to the greater heating of the magnetodisc plasma at dusk
 73 compared to dawn (Kaminker et al., 2017) and the expansion of the magnetic field as
 74 it rotates from noon through dusk, resulting in instabilities arising in the disc. We fur-
 75 ther compare the region at which magnetodisc breakdown is expected to occur and find
 76 it is on average within the magnetosphere of Jupiter but not Saturn, possibly explain-
 77 ing the difference between these two systems.

78 2 Data Selection

79 To search for a cushion region at Saturn, all Cassini orbits that traversed the day-
 80 side inner magnetosphere out to the magnetopause, whilst remaining near the equator
 81 ($\pm 30^\circ$) are analysed to track how the magnetic field configuration changes with radial
 82 distance. Crossings of the dayside magnetopause are identified using the Jackman et al.
 83 (2019) catalogue. The standoff distance R_{SS} for each unique crossing, using the first or
 84 last crossing if there are multiple during a single traversal, is mapped with the Pilkington
 85 et al. (2015) dawn-dusk asymmetric magnetopause model. The local time correction in-
 86 troduces a maximum $\pm 0.5R_S$ difference in R_{SS} compared to an axisymmetric model,
 87 but it is included for completeness. There are 93 suitable revolutions (Revs) from the
 88 mission that fulfil the above criteria and are shown in Figure 1.

89 The 1-minute resolution magnetometer data is transformed into Kronocentric So-
 90 lar Magnetic (KSMAG) spherical coordinates, where r is the radial component and posi-
 91 tive pointing away from Saturn, θ is the north-south meridional component and ϕ is the
 92 azimuthal component increasing in the direction of rotation. An 11-hour (approximate
 93 rotation period) sliding average of the data is taken to focus on the global structure and
 94 filter other variability, including the ubiquitous planetary period oscillations (PPOs) (see
 95 (Carbary & Mitchell, 2013) review and references therein).

96 3 Finding the Cushion Region

97 To identify whether a cushion exists, there must be a stable disc structure in the
 98 middle to outer magnetosphere, otherwise the field could be quasi-dipolar everywhere.
 99 There are two conditions for the magnetic field to be disc-like (Went, Kivelson, et al.,
 100 2011). Firstly, the field must be predominantly radial such that $B_r^2/B^2 > B_\theta^2/B^2$. These
 101 ratios are shown in panels b) and e) of Figure 2. However, this criterion is insufficient
 102 when Cassini is away from the equator, where a dipole field is not purely north-south.
 103 This is particularly important to consider if the current sheet is warped (Arridge, Khu-
 104 rana, et al., 2008). To account for this, the second criterion is for the angle between the
 105 measured magnetic field and a dipole, where we have used the Dougherty et al. (2018)
 106 model, to be $90 \pm 30^\circ$. This angle is shown in panels c) and f) of Figure 2. When both
 107 these criteria are satisfied, we suggest that the field is disk-like.

108 The location 80% of the distance from the $15R_S$ disc inner edge to the magnetopause
 109 is set as the cushion region inner edge. For instance, if the magnetopause radial posi-
 110 tion is $r = 25R_S$ the cushion inner edge is $r = 23R_S$. Whilst this is closer to the mag-

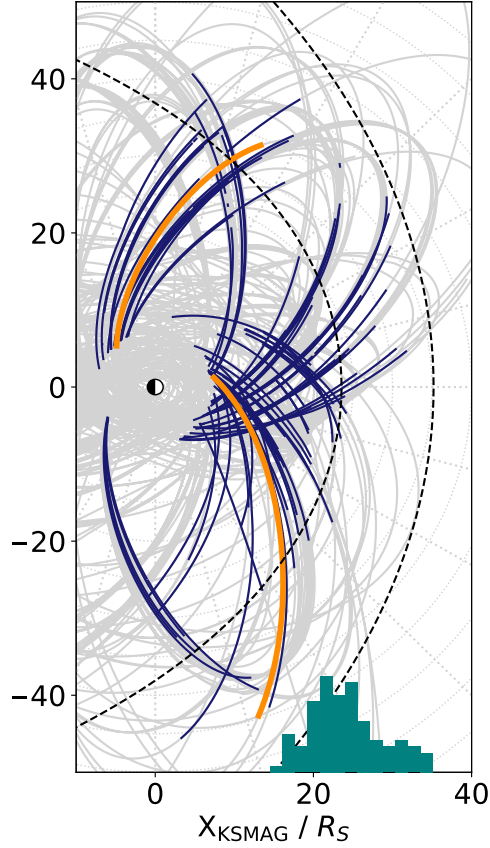


Figure 1. The complete Cassini orbital mission trajectory is shown in light grey, projected onto the equatorial plane, where the Sun is to the right. The trajectory of Cassini during the 93 Revs used in this study is shown in dark blue, where the crossing of the magnetopause occurred at the furthest radial distance on each path. The orange trajectories show the case studies in Figure 2. Magnetopause (Pilkington et al., 2015) and bow shock (Went, Hospodarsky, et al., 2011) models, assuming solar wind dynamic pressure of 0.01 nPa, are shown with black dashed curves. The histogram shows R_{SS} for each crossing.

111 netopause than the average inner boundary of the Jovian cushion (Went, Kivelson, et
 112 al., 2011), it is chosen due to the lack of an observed cushion thus far and the smaller
 113 magnetosphere of Saturn. It is also far enough from the magnetopause to assume we are
 114 not just measuring the shielding of the field by the boundary currents, although previ-
 115 ous evidence of the disc persisting up to the magnetopause (Arridge, Russell, et al., 2008)
 116 shows that this effect should be negligible. We then calculate what percentage of the data
 117 fulfil the two criteria in the disc region (from $15R_S$ to the cushion inner edge). If it is
 118 more than 50%, we suggest that there exists a stable magnetodisc structure. In the cush-
 119 ion region (the remaining radial distance to the magnetopause), if this percentage remains
 120 approximately constant, the field has remained disc-like. If the percentage significantly
 121 reduces and the field becomes more dipolar, there is a cushion. If less than 50% of the

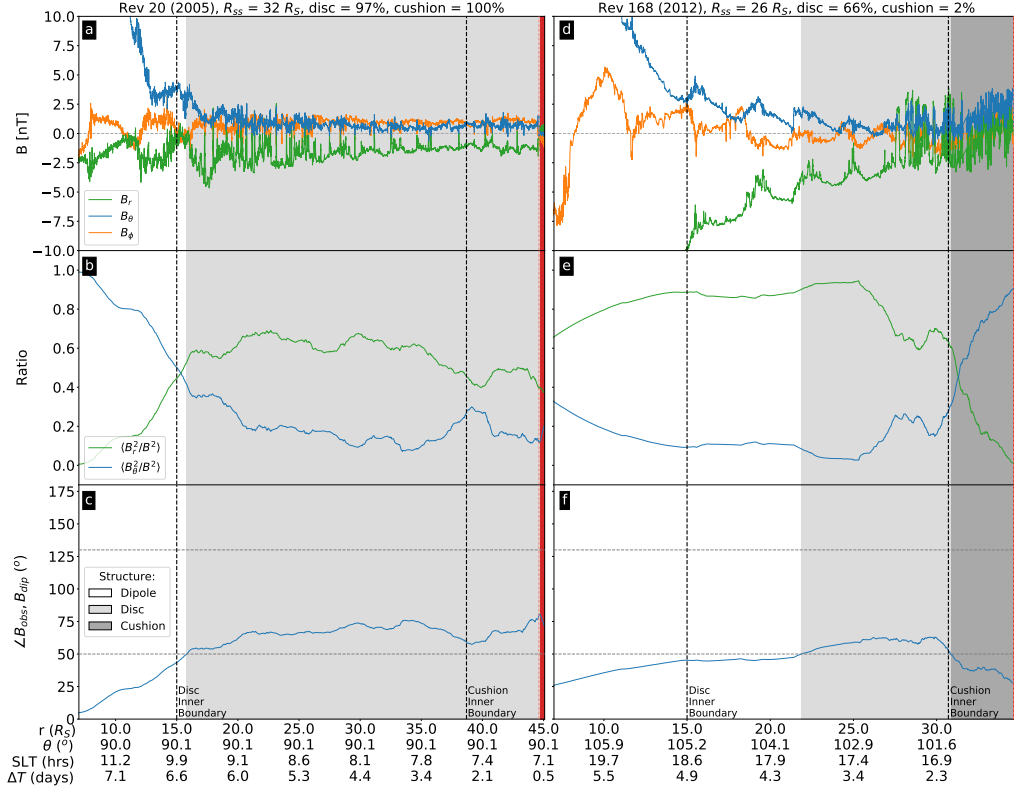


Figure 2. Two example where Cassini traversed the equatorial dayside magnetosphere of Saturn are shown as a function of radial distance. Both examples are inbound, where the time since magnetopause crossing ΔT is increasing as you move towards the planet (increasing from right to left). The top panels show the 1-minute resolution magnetic field in spherical KSMAG coordinates. The second panels show the ratio of the 11-hour smoothed radial and meridional components to the total field. The bottom panels show the angle between the measured field and the Dougherty et al. (2018) internal magnetic field model. These two quantities identify whether the disc criteria are satisfied. The panels are shaded to show if the field is dipole-like (white), disc-like (light grey), cushion-like (dark grey), or in the magnetosheath (red). The disc and cushion region boundaries are shown as vertical dashed lines. The left panels show an example at dawn where the magnetodisc is present up until the magnetopause, whilst the right panels show an example at dusk where a cushion is identified. At the bottom of the figure the radial distance (r), co-latitude (θ), Saturn local time (SLT), and ΔT are shown.

122 disc region has fulfilled the criteria, there is no stable magnetodisc and so we cannot check
 123 whether there is a cushion present. This ensures we see two distinct regions with per-
 124 sistent and sustained structures.

125 The change in percentage across these two regions for all 93 Revs was then calcu-
 126 lated. The mean change in percentage was a reduction by $\mu = 6\%$ with a standard de-
 127 viation of $\sigma = 24\%$. We define those Revs whose reduction in percentage is greater than
 128 $\mu + 2\sigma = 54\%$ as having a cushion. The reduction in percentage is large enough to con-
 129 sider these as examples of a cushion and not an artefact of our method, compared to if,
 130 for instance, $\mu + 2\sigma$ was only 10% reduction.

131

3.1 Results

132

133

134

135

136

137

138

139

For Rev 20 in the left panels of Figure 2, the disc criteria are satisfied for 97% of the disc region and for 100% of the cushion region, showing an example of a stable magnetodisc structure that persists up to the magnetopause. The mapped standoff distance R_{SS} for Rev 20 was $32R_S$, showing that the system was significantly expanded. For Rev 168, the criteria are satisfied for 66% of the disc region. However, the percentage drops to just 2% in the cushion region and the field becomes significantly more dipolar. For Rev 168, $R_{SS} = 26R_S$, showing the system was in an expanded state. We suggest that this is the first evidence of a cushion region observed at Saturn.

140

141

142

143

144

145

146

147

148

149

150

151

152

A potential explanation for the Rev 168 cushion region could be that the dipolar outer boundary reflects the change in local time as Cassini moves away from noon (in time) and the magnetopause confinement of the field reduces. However, Cassini only passed through 0.2 hours of local time in the cushion region, and 1.2 hours between where the disc was first observed and the cushion region inner edge, producing a small change in the magnetopause radial position. In addition, Revs with a similar noonward trajectory where a disc was observed at dawn did not observe a dipolar outer region. Another explanation could be that the magnetosphere underwent a sudden solar wind compression. Whilst for the Rev 168 there is a small increase in magnetic field strength (~ 1 nT), the data are particularly noisy in this region and the cushion was observed radially inwards of this small increase. In addition, we compared the field profile for all six potential examples of a cushion region (see Figure 3) and saw no significant increase in field strength to suggest that these are results of a solar wind compression.

153

154

155

156

157

158

159

This analysis was carried out for all 93 Revs. Only 15 Revs had a sustained magnetodisc and are shown in Figure 3a) in grey. The disc formed not only when the magnetosphere was expanded ($R_{SS} > 24R_S$), but even when R_{SS} was as low as $17R_S$. Of these 15 Revs, five contain potential examples of cushion regions and are highlighted in Figure 3a). For all cushion region examples, the mapped magnetopause standoff distance was greater than $24R_S$. However, a cushion does not arise whenever the magnetosphere is expanded. In particular, it does not arise preferentially at dawn as was expected.

160

161

162

163

164

165

166

167

168

169

170

In panel b) of Figure 3, the average magnetic field structure calculated using this subset of 15 Revs with a sustained magnetodisc is shown, revealing a local time asymmetry. When there is a magnetodisc at dawn, the structure is stable in the disc region (median of 95% for nine Revs) and this continues into the presumed cushion region (median of 100%). At dusk, when there is a magnetodisc it is on average less stable in the disc region (median of 68% for six Revs) and this significantly drops in the cushion region (median of 1%). One example was found of a stable disc that persists up to the magnetopause at dusk, compared to eight at dawn. Of the five examples of a cushion region found at Saturn, four are at dusk and one is at dawn. This result is unexpected if we assume the cushion region is a return flow channel of mass depleted flux tubes following large-scale reconnection in the tail.

171

172

173

174

175

176

177

For this study, the focus is on whether a significant portion of the outer boundary is persistently dipolar, reflective of the cushion region that has been observed at Jupiter, rather than being intermittently dipolar. We have taken an 11-hour average of the magnetic field data to focus on the large-scale properties of the magnetic field structure. Some examples of what appear to be signatures of an intermittent cushion were therefore removed from our analysis. We found that the overall structure at dusk is far noisier, which is reflected in the low disc region percentage at dusk in Figure 3.

178

4 Discussion

179

180

The magnetodisc structure maintains an equilibrium between the outward directed centrifugal force, the magnetic and plasma pressures, and the magnetic field tension in

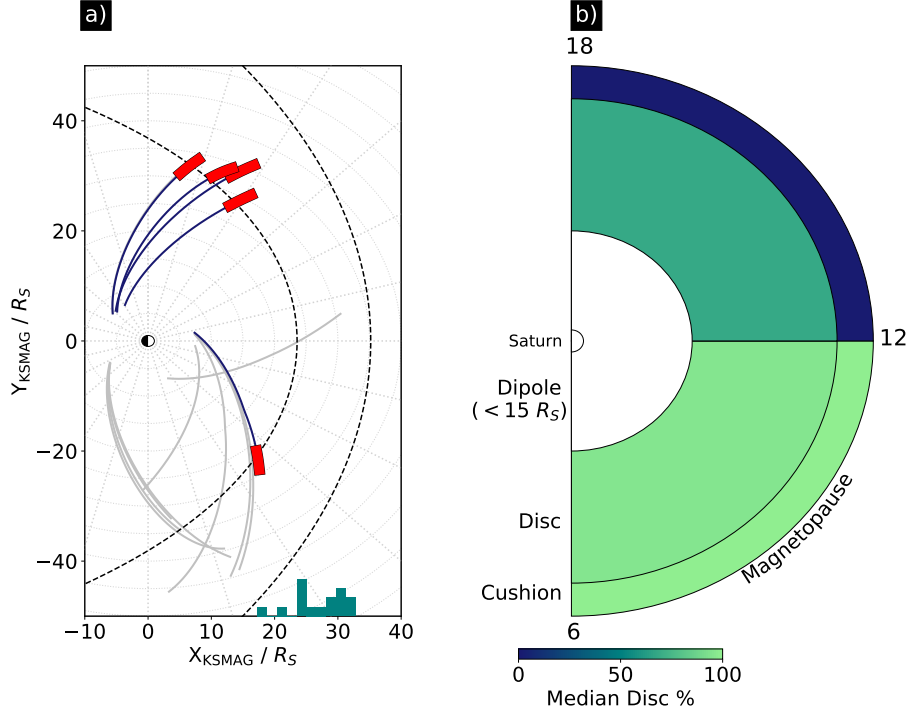


Figure 3. Panel a) shows the Cassini trajectories in a similar format to Figure 1, but only the 15 Cassini Revs where a stable disc was identified are shown in grey. The five cushion examples are shown in blue, with the cushion highlighted in red. There is one example of a disc with no cushion at dusk, but its trajectory is underneath a cushion case. Panel b) shows a representation of the average dayside configuration calculated using the 15 examples in panel a). The three radial sectors of dipole, disc and cushion are labelled and the dayside is divided into dawn and dusk local time sectors. The colorbar shows the median disc percentage. There is a distinct disc structure at dawn that persists up to the magnetopause (light green). At dusk, on average there is a less stable disc in the disc region (dark green). The field structure becomes less disc-like in the cushion region (blue), showing evidence for a dipole cushion structure at dusk.

181 the curved geometry that provides the inward centripetal force required to enforce sub-
 182 corotation. The field radius of curvature R_C supports this equilibrium. Magnetodisc break-
 183 down can occur when this radial stress balance is disrupted and the magnetic field can
 184 no longer contain the plasma. Ballooning of the disc is expressed by the plasma paral-
 185 lel pressure being greater than the perpendicular pressure plus the magnetic tension as-
 186 sociated with the curved field geometry. This instability can therefore lead to reconec-
 187 tion and plasma breaking off the disc. To identify where the force balance in the disc might
 188 break down, we can compare the gyroradii of plasma ions to identify where it approaches
 189 the length-scale R_C that is associated with maintaining the disc structure. The typical
 190 ion gyroradius of a charged particle can be expressed as

$$r_i = \frac{\sqrt{2mk_bT}}{|q|B} \quad (1)$$

191 where m is the particle mass, q is the charge, B is the local magnetic field strength, T
 192 is the temperature (where we assume that $T_{\perp} \approx T$) and where k_b is the Boltzmann con-
 193 stant. Went, Kivelson, et al. (2011) calculated the critical density in the disc under which

194 stress balance would break down. However, due to a lack of data close to the magnetopause
 195 at Saturn they could not resolve this difference between the gas giants. Now the Cassini
 196 mission is complete, we can build on their work using the latest results to understand
 197 these new cushion observations.

198 We calculate magnetic field profiles using the complete Cassini (Dougherty et al.,
 199 2004) and Galileo (Kivelson et al., 1992) magnetometer datasets. We fit a power-law model
 200 to the increasing thermal heavy ion temperatures observed at Saturn (Wilson et al., 2017)
 201 and Jupiter (Kim et al., 2020). For both planets we assume a mass-per-charge ratio of
 202 16 for the magnetodisc plasma, assuming it is dominated by O^+ at Saturn and is a com-
 203 bination of O^+ and S^{2+} at Jupiter. An expanded magnetosphere is also assumed, with
 204 $R_{SS} = 24R_S$ for Saturn and $R_{SS} = 75R_J$ for Jupiter.

205 Plugging these into Equation 1, we get one-dimensional gyroradii profiles as a func-
 206 tion of radial distance shown in Figure 4. Both show an increase in gyroradius as a func-
 207 tion of radial distance, going from 10^1 kilometres in the inner magnetosphere to 10^3 kilo-
 208 metres at the magnetopause standoff distance, and finally to 10^4 kilometres close to the
 209 dawn terminator.

210 To calculate R_C at both Saturn and Jupiter, we use the AGA/UCL Magnetodisc
 211 Model (Achilleos et al., 2010) assuming an average hot plasma index for both planets
 212 ($K_h = 2e6 \text{ Pa m T}^{-1}$ and $K_h = 3e7 \text{ Pa m T}^{-1}$ for Saturn and Jupiter, respectively,
 213 where K_h is essentially a measure of the ring current activity). For Saturn, the small-
 214 est value of R_C calculated in the middle magnetosphere was $\sim 0.70R_S$, and for Jupiter
 215 it was $\sim 0.64R_J$. For comparison, we include $R_C \sim 0.40R_J$ in the middle magnetosphere
 216 of Jupiter given by the (Nichols et al., 2015) force balance model.

217 Figure 4 shows that at Jupiter the gyroradius of the heavy ion population that dom-
 218 inates the magnetodisc current sheet is more likely, both in the average case and more
 219 so in disturbed conditions (lower field strength, higher temperature) to approach the ex-
 220 pected radius of curvature. Past this region, the magnetohydrodynamic approximation
 221 of the magnetodisc breaks down and force balance is no longer maintained. Ballooning
 222 of the field that allows plasma to break off the disc has been identified at Jupiter (Haynes
 223 et al., 1994; Southwood et al., 1995) along with the sustained cushion region observed
 224 by Went, Kivelson, et al. (2011) in the approximate radial regions shown in Figure 4.

225 At Saturn, other than in perhaps the most disturbed conditions, it is unlikely to
 226 see the disc stress balance breakdown, as is observed in Figure 4. Kaminker et al. (2017)
 227 identified the noon to dusk sectors (10-20 LT) as having a greater heater rate density,
 228 calculated using fluctuations in the magnetic field. Greater heating of the magnetodisc
 229 plasma would imply a larger r_i at dusk, where the plasma could be heated and escape
 230 down the tail. There is also an asymmetry in the hot plasma pressure, which is larger
 231 at dusk compared to dawn (Sergis et al., 2017; Sorba et al., 2019). Delamere et al. (2015)
 232 found evidence of mass being lost from the disc through signatures of reconnection, given
 233 by $B_\theta < 0$, predominantly in the subsolar to dusk regions. Although it should be noted
 234 that this single criterion cannot distinguish a bent magnetic field configuration, for in-
 235 stance through solar wind driven warping. Nonetheless, they suggest a circulation pat-
 236 tern in the magnetodisc where mass is lost through patchy reconnection in the dusk flank,
 237 rather than through large-scale tail reconnection. As flux tubes rotates through dusk they
 238 are able to expand since the magnetopause no longer confines the field, resulting in a cen-
 239 trifugally driven increase in the parallel pressure of the plasma. This develops an anisotropy
 240 ($T_{\parallel} > T_{\perp}$) that results in the disc becoming explosively unstable at dusk (Kivelson & South-
 241 wood, 2005). There could also be a further role of the solar wind and the Dungey cy-
 242 cle (Dungey, 1961) in the dusk cushion formation, as well as the planetary period oscil-
 243 lations that thin the current sheet (Cowley et al., 2017).

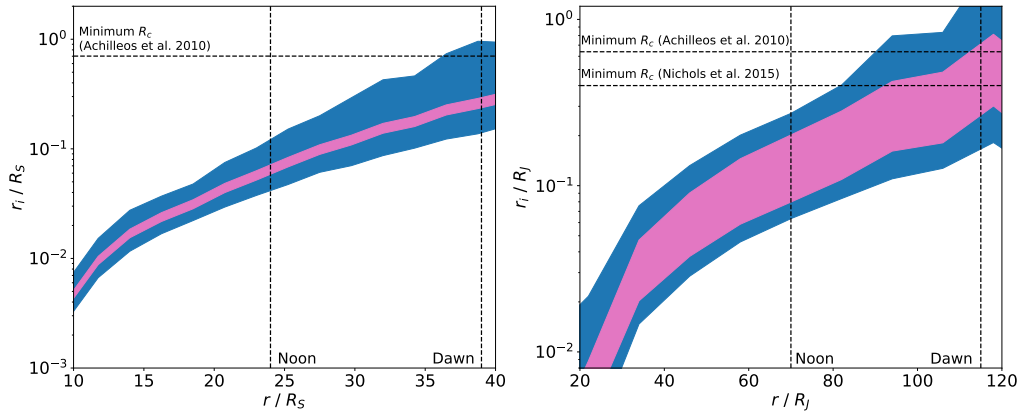


Figure 4. The gyroradius r_i of heavy ions ($\text{amu}/q \approx 16$ for both planets) that dominate the magnetodisc current sheets at Saturn (left) and Jupiter (right), shown as a function of radial distance in units of planetary radii. The horizontal dashed lines show the minimum R_C in the middle magnetosphere given by the Achilleos et al. (2010); Nichols et al. (2015) magnetodisc models. The vertical dashed lines show the magnetopause radial distance at noon and the mapped dawn terminator using the Pilkington et al. (2015) model. We assume an expanded state for both systems, with $R_{SS} = 24R_S$ for Saturn and $R_{SS} = 75R_J$ for Jupiter. The pink region shows r_i calculated using the average magnetic field strength, where the width represents errors in the fitted temperature models. The blue region shows r_i calculated using the standard deviations of the mean magnetic field, highlighting the variability, particularly close to the magnetopause boundary. These results show that r_i approaches R_C at Jupiter at distances between the noon and dawn magnetopause both in the average and perturbed cases, but at Saturn it is less likely for this to occur.

244 In this study, we have observed cases where the dipolar structure associated with
 245 plasma being absent or depleted from the equatorial region persists throughout the cush-
 246 ion region. However, this large-scale structure rarely occurs and instead small-scale sig-
 247 natures of a patchy cushion and an unstable disc are more commonly observed at dusk
 248 (e.g. Delamere et al. (2015)).

249 Pulsations in the ultraviolet (UV) auroral emissions have further been linked with
 250 magnetodisc reconnection and are observed to preferentially occur at dusk with patchy,
 251 diffuse signatures (Bader et al., 2019, 2020). These phenomena highlight the quieter dawn
 252 magnetodisc that maps to the aurora along field-aligned currents compared to the active
 253 and more variable dusk magnetodisc and cushion that generate these structures.

254 We have further compared the effect of the suprathermal ions on the magnetic field
 255 structure near the boundary (see Supplementary Information). We would expect their
 256 presence in the outer magnetosphere to produce a more dipolar structure, an effect ob-
 257 served in magnetodisc models that incorporate hot plasma (e.g. (Caudal, 1986; Achilleos
 258 et al., 2010; Nichols et al., 2015)). Under certain circumstances this effect could be re-
 259 levant, but for average conditions we suggest magnetodisc breakdown more clearly de-
 260 scribes the formation of the cushion region.

261 5 Conclusion

262 Using the complete Cassini orbital magnetometer dataset, we have identified five
 263 examples of a cushion region at Saturn, of which four were observed at dusk. These re-

264 sults are in contrast with the current interpretation of a cushion that suggests it is a re-
 265 turn flow channel of mass depleted flux tubes following tail reconnection. We suggest that
 266 the cushion region is more likely to form at Jupiter primarily due to the larger system
 267 size that allows for a breakdown of the magnetodisc. At Saturn, this is less likely to oc-
 268 cur except under certain circumstances, such as greater heating. Due to a local time asym-
 269 metry in the heating of the plasma and the expansion of the field as the plasma rotates
 270 through the afternoon sector, the dusk magnetodisc is more likely to undergo these in-
 271 stabilities, allowing for a cushion region to form preferentially in this local time sector.

272 Acknowledgments

273 N. R. S. is funded by the STFC DTP Studentship. M. K. D. is supported by a Royal
 274 Society Research Professorship. A. M. is supported by a Royal Society University Re-
 275 search Fellowship. N. A. was supported by the UK STFC Consolidated Grant (UCL/MSSL
 276 Solar and Planetary Physics, ST/N000722/1). The calibrated 1 min resolution Cassini
 277 magnetic field data in KSM coordinates are available at the Planetary Plasma Interac-
 278 tion (PPI) Node of NASA’s Planetary Data System (PDS) (<https://pds-ppi.igpp.ucla.edu/>)
 279 in the folder CO-E/SW/J/SMAG-4-SUMM-1MINAVG-V2.0. We would like to thank
 280 David Southwood for his insightful discussions.

281 References

- 282 Achilleos, N., Guio, P., & Arridge, C. S. (2010, Feb). A model of force balance
 283 in saturn’s magnetodisc. *Monthly Notices of the Royal Astronomical So-*
 284 *ciety*, *401*(4), 2349–2371. Retrieved from [http://dx.doi.org/10.1111/](http://dx.doi.org/10.1111/j.1365-2966.2009.15865.x)
 285 [j.1365-2966.2009.15865.x](http://dx.doi.org/10.1111/j.1365-2966.2009.15865.x) doi: 10.1111/j.1365-2966.2009.15865.x
- 286 Arridge, C. S., Khurana, K. K., Russell, C. T., Southwood, D. J., Achilleos, N.,
 287 Dougherty, M. K., ... Leinweber, H. K. (2008). Warping of Saturn’s magne-
 288 topheric and magnetotail current sheets. *Journal of Geophysical Research:*
 289 *Space Physics*, *113*(8), 1–13. doi: 10.1029/2007JA012963
- 290 Arridge, C. S., Russell, C. T., Khurana, K. K., Achilleos, N., Cowley, S. W.,
 291 Dougherty, M. K., ... Bunce, E. J. (2008). Saturn’s magnetodisc current
 292 sheet. *Journal of Geophysical Research: Space Physics*, *113*(4), 1–9. doi:
 293 10.1029/2007JA012540
- 294 Bader, A., Badman, S. V., Yao, Z. H., Kinrade, J., & Pryor, W. R. (2019). Ob-
 295 servations of Continuous Quasiperiodic Auroral Pulsations on Saturn in High
 296 Time-Resolution UV Auroral Imagery. *Journal of Geophysical Research: Space*
 297 *Physics*, *124*(4), 2451–2465. doi: 10.1029/2018JA026320
- 298 Bader, A., Cowley, S. W., Badman, S. V., Ray, L. C., Kinrade, J., Palmaerts, B.,
 299 & Pryor, W. R. (2020). The Morphology of Saturn’s Aurorae Observed
 300 During the Cassini Grand Finale. *Geophysical Research Letters*, *47*(2). doi:
 301 10.1029/2019GL085800
- 302 Carbary, J. F., & Mitchell, D. G. (2013). Periodicities in saturn’s magne-
 303 tosphere. *Reviews of Geophysics*, *51*(1), 1-30. Retrieved from [https://](https://agupubs.onlinelibrary.wiley.com/doi/abs/10.1002/rog.20006)
 304 agupubs.onlinelibrary.wiley.com/doi/abs/10.1002/rog.20006 doi:
 305 10.1002/rog.20006
- 306 Caudal, G. (1986). A self-consistent model of jupiter’s magnetodisc includ-
 307 ing the effects of centrifugal force and pressure. *Journal of Geophysical*
 308 *Research: Space Physics*, *91*(A4), 4201-4221. Retrieved from [https://](https://agupubs.onlinelibrary.wiley.com/doi/abs/10.1029/JA091iA04p04201)
 309 agupubs.onlinelibrary.wiley.com/doi/abs/10.1029/JA091iA04p04201
 310 doi: 10.1029/JA091iA04p04201
- 311 Cowley, S. W., Provan, G., Hunt, G. J., & Jackman, C. M. (2017). Planetary pe-
 312 riod modulations of Saturn’s magnetotail current sheet: A simple illustrative
 313 mathematical model. *Journal of Geophysical Research: Space Physics*, *122*(1),
 314 258–279. doi: 10.1002/2016JA023367

- 315 Delamere, P. a., Otto, a., Ma, X., Bagenal, F., & Wilson, R. J. (2015). *Journal of Geophysical Research : Space Physics* Magnetic flux circulation in
 316 the rotationally driven giant magnetospheres. , 4229–4245. doi: 10.1002/
 317 2015JA021036. Received
 318
- 319 Dougherty, M., Cao, H., Khurana, K., Hunt, G., Provan, G., Kellock, S., ... South-
 320 wood, D. (2018). Saturn’s magnetic field revealed by the cassini grand fi-
 321 nale (vol 362, eaat5434, 2018). *SCIENCE*, 362. Retrieved from [http://](http://dx.doi.org/10.1126/science.aav6732)
 322 dx.doi.org/10.1126/science.aav6732 doi: 10.1126/science.aav6732
- 323 Dougherty, M., Kellock, S., Southwood, D. J., Balogh, A., Smith, E. J., Tsuru-
 324 tani, B. T., ... Cowley, S. W. H. (2004). The Cassini Magnetic Field
 325 Investigation. *The Cassini-Huygens Mission*, 331–383. Retrieved from
 326 [http://link.springer.com/10.1007/978-1-4020-2774-1{_}4](http://link.springer.com/10.1007/978-1-4020-2774-1_{_}4) doi:
 327 10.1007/978-1-4020-2774-1.4
- 328 Dungey, J. W. (1961). Interplanetary magnetic field and the auroral zones. *Physical*
 329 *Review Letters*, 6(2), 47–48. doi: 10.1103/PhysRevLett.6.47
- 330 Gershman, D. J., DiBraccio, G. A., Connerney, J. E., Bagenal, F., Kurth, W. S.,
 331 Hospodarsky, G. B., ... Bolton, S. J. (2018). Juno Constraints on the For-
 332 mation of Jupiter’s Magnetospheric Cushion Region. *Geophysical Research*
 333 *Letters*, 45(18), 9427–9434. doi: 10.1029/2018GL079118
- 334 Gold, T. (1959). Motions in the magnetosphere of the earth. *Journal of Geo-*
 335 *physical Research (1896-1977)*, 64(9), 1219–1224. Retrieved from [https://](https://agupubs.onlinelibrary.wiley.com/doi/abs/10.1029/JZ064i009p01219)
 336 agupubs.onlinelibrary.wiley.com/doi/abs/10.1029/JZ064i009p01219
 337 doi: 10.1029/JZ064i009p01219
- 338 Haynes, P. L., Balogh, A., Dougherty, M. K., Southwood, D. J., Fazakerley, A., &
 339 Smith, E. J. (1994). Null fields in the outer jovian magnetosphere: Ulysses
 340 observations. *Geophysical Research Letters*, 21(6), 405–408. Retrieved from
 341 <https://agupubs.onlinelibrary.wiley.com/doi/abs/10.1029/93GL01986>
 342 doi: 10.1029/93GL01986
- 343 Jackman, C. M., Thomsen, M. F., & Dougherty, M. K. (2019). Survey of Saturn’s
 344 Magnetopause and Bow Shock Positions Over the Entire Cassini Mission:
 345 Boundary Statistical Properties and Exploration of Associated Upstream Con-
 346 ditions. *Journal of Geophysical Research: Space Physics*, 124(11), 8865–8883.
 347 doi: 10.1029/2019JA026628
- 348 Jasinski, J. M., Arridge, C. S., Bader, A., Smith, A. W., Felici, M., Kinrade, J., ...
 349 Murphy, N. (2019). Saturn’s Open-Closed Field Line Boundary: A Cassini
 350 Electron Survey at Saturn’s Magnetosphere. *Journal of Geophysical Research:*
 351 *Space Physics*, 124(12), 10018–10035. doi: 10.1029/2019JA027090
- 352 Kaminker, V., Delamere, P. A., Ng, C. S., Dennis, T., Otto, A., & Ma, X. (2017).
 353 Local time dependence of turbulent magnetic fields in Saturn’s magnetodisc.
 354 *Journal of Geophysical Research: Space Physics*, 122(4), 3972–3984. doi:
 355 10.1002/2016JA023834
- 356 Kim, T. K., Ebert, R. W., Valek, P. W., Allegrini, F., McComas, D. J., Bagenal, F.,
 357 ... Bolton, S. J. (2020). Survey of Ion Properties in Jupiter’s Plasma Sheet:
 358 Juno JADE-I Observations. *Journal of Geophysical Research: Space Physics*,
 359 125(4), 1–21. doi: 10.1029/2019ja027696
- 360 Kivelson, M. G., Khurana, K. K., Means, J. D., Russell, C. T., & Snare, R. C.
 361 (1992). The Galileo magnetic field investigation. *Space Science Reviews*,
 362 60(1-4), 357–383. doi: 10.1007/BF00216862
- 363 Kivelson, M. G., & Southwood, D. J. (2005). Dynamical consequences of two modes
 364 of centrifugal instability in Jupiter’s outer magnetosphere. *Journal of Geophys-*
 365 *ical Research: Space Physics*, 110(A12). doi: 10.1029/2005JA011176
- 366 Masters, A., Thomsen, M. F., Badman, S. V., Arridge, C. S., Young, D. T., Coates,
 367 A. J., & Dougherty, M. K. (2011). Supercorotating return flow from reconec-
 368 tion in Saturn’s magnetotail. *Geophysical Research Letters*, 38(3), 3–7. doi:
 369 10.1029/2010GL046149

- 370 Nichols, J. D., Achilleos, N., & Cowley, S. W. (2015). A model of force balance
 371 in Jupiter's magnetodisc including hot plasma pressure anisotropy. *Jour-*
 372 *nal of Geophysical Research: Space Physics*, *120*(12), 10185–10206. doi:
 373 10.1002/2015JA021807
- 374 Pilkington, N. M., Achilleos, N., Arridge, C. S., Guio, P., Masters, A., Ray, L. C.,
 375 ... Dougherty, M. K. (2015). Asymmetries observed in Saturn's magne-
 376 topause geometry. *Geophysical Research Letters*, *42*(17), 6890–6898. doi:
 377 10.1002/2015GL065477
- 378 Sergis, N., Jackman, C. M., Thomsen, M. F., Krimigis, S. M., Mitchell, D. G.,
 379 Hamilton, D. C., ... Wilson, R. J. (2017). Radial and local time structure
 380 of the Saturnian ring current, revealed by Cassini. *Journal of Geophysical*
 381 *Research: Space Physics*, *122*(2), 1803–1815. doi: 10.1002/2016JA023742
- 382 Sorba, A. M., Achilleos, N. A., Sergis, N., Guio, P., Arridge, C. S., & Dougherty,
 383 M. K. (2019). Local time variation in the large-scale structure of saturn's
 384 magnetosphere. *Journal of Geophysical Research: Space Physics*, *124*(9), 7425-
 385 7441. Retrieved from [https://agupubs.onlinelibrary.wiley.com/doi/abs/](https://agupubs.onlinelibrary.wiley.com/doi/abs/10.1029/2018JA026363)
 386 [10.1029/2018JA026363](https://agupubs.onlinelibrary.wiley.com/doi/abs/10.1029/2018JA026363) doi: 10.1029/2018JA026363
- 387 Southwood, D., Dougherty, M., Leamon, R., & Haynes, P. (1995). Origin and dy-
 388 namics of field nulls detected in the jovian magnetospheres. *Advances in Space*
 389 *Research*, *16*(4), 177 - 181. Retrieved from [http://www.sciencedirect.com/](http://www.sciencedirect.com/science/article/pii/0273117795002265)
 390 [science/article/pii/0273117795002265](http://www.sciencedirect.com/science/article/pii/0273117795002265) (Comparative Studies of Magneto-
 391 spheric Phenomena) doi: [https://doi.org/10.1016/0273-1177\(95\)00226-5](https://doi.org/10.1016/0273-1177(95)00226-5)
- 392 Vasyliunas, V. M. (1983). Plasma distribution and flow. In *Physics of the jo-*
 393 *vian magnetosphere* (p. 395-453). Cambridge University Press. doi: 10.1017/
 394 CBO9780511564574.013
- 395 Went, D. R., Hospodarsky, G. B., Masters, A., Hansen, K. C., & Dougherty, M. K.
 396 (2011). A new semiempirical model of Saturn's bow shock based on propa-
 397 gated solar wind parameters. *Journal of Geophysical Research: Space Physics*,
 398 *116*(7), 1–9. doi: 10.1029/2010JA016349
- 399 Went, D. R., Kivelson, M. G., Achilleos, N., Arridge, C. S., & Dougherty, M. K.
 400 (2011). Outer magnetospheric structure: Jupiter and Saturn compared.
 401 *Journal of Geophysical Research: Space Physics*, *116*(4), 1–14. doi:
 402 10.1029/2010JA016045
- 403 Wilson, R. J., Bagenal, F., & Persoon, A. M. (2017). Survey of thermal plasma ions
 404 in Saturn's magnetosphere utilizing a forward model. *Journal of Geophysical*
 405 *Research: Space Physics*, *122*(7), 7256–7278. doi: 10.1002/2017JA024117
- 406 Young, D. T., Berthelier, J. J., Blanc, M., Burch, J. L., Coates, A. J., Goldstein, R.,
 407 ... Zinsmeyer, C. (2004, Sep 01). Cassini plasma spectrometer investigation.
 408 *Space Science Reviews*, *114*(1), 1–112. Retrieved from [https://doi.org/](https://doi.org/10.1007/s11214-004-1406-4)
 409 [10.1007/s11214-004-1406-4](https://doi.org/10.1007/s11214-004-1406-4) doi: 10.1007/s11214-004-1406-4

Figure 1.

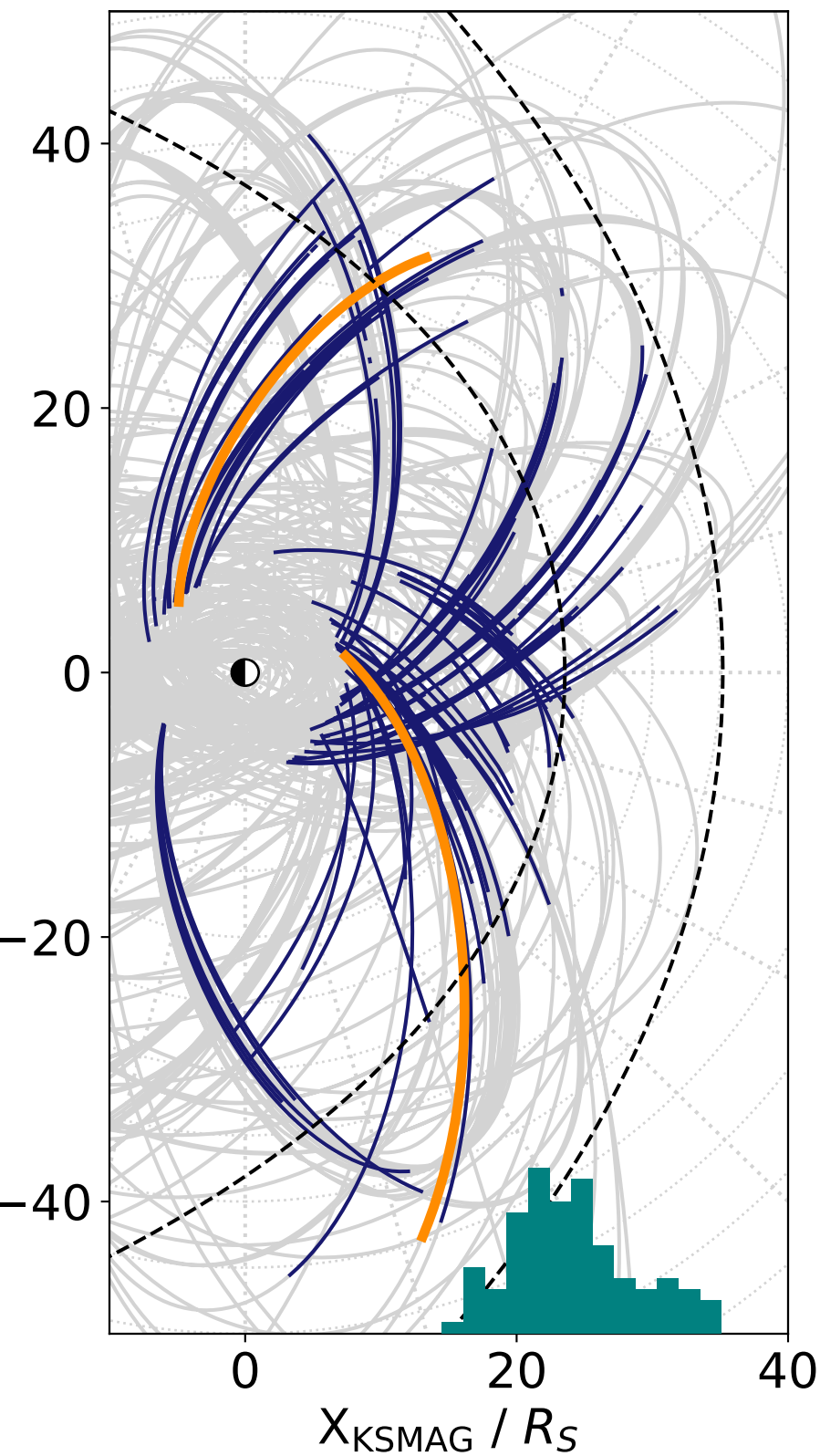


Figure 2.

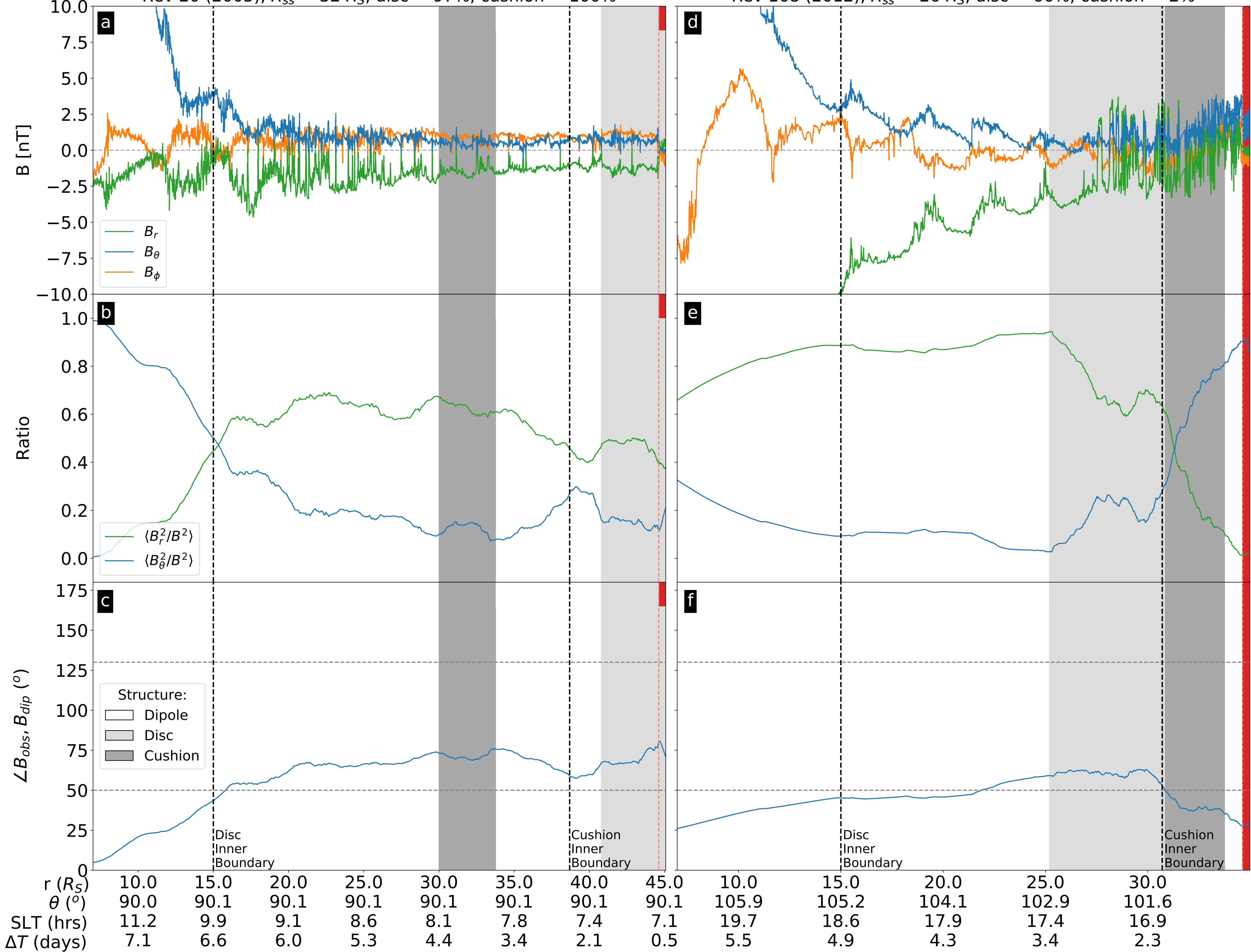
Rev 20 (2005), $R_{SS} = 32 R_S$, disc = 97%, cushion = 100%Rev 168 (2012), $R_{SS} = 26 R_S$, disc = 66%, cushion = 2%

Figure 3.

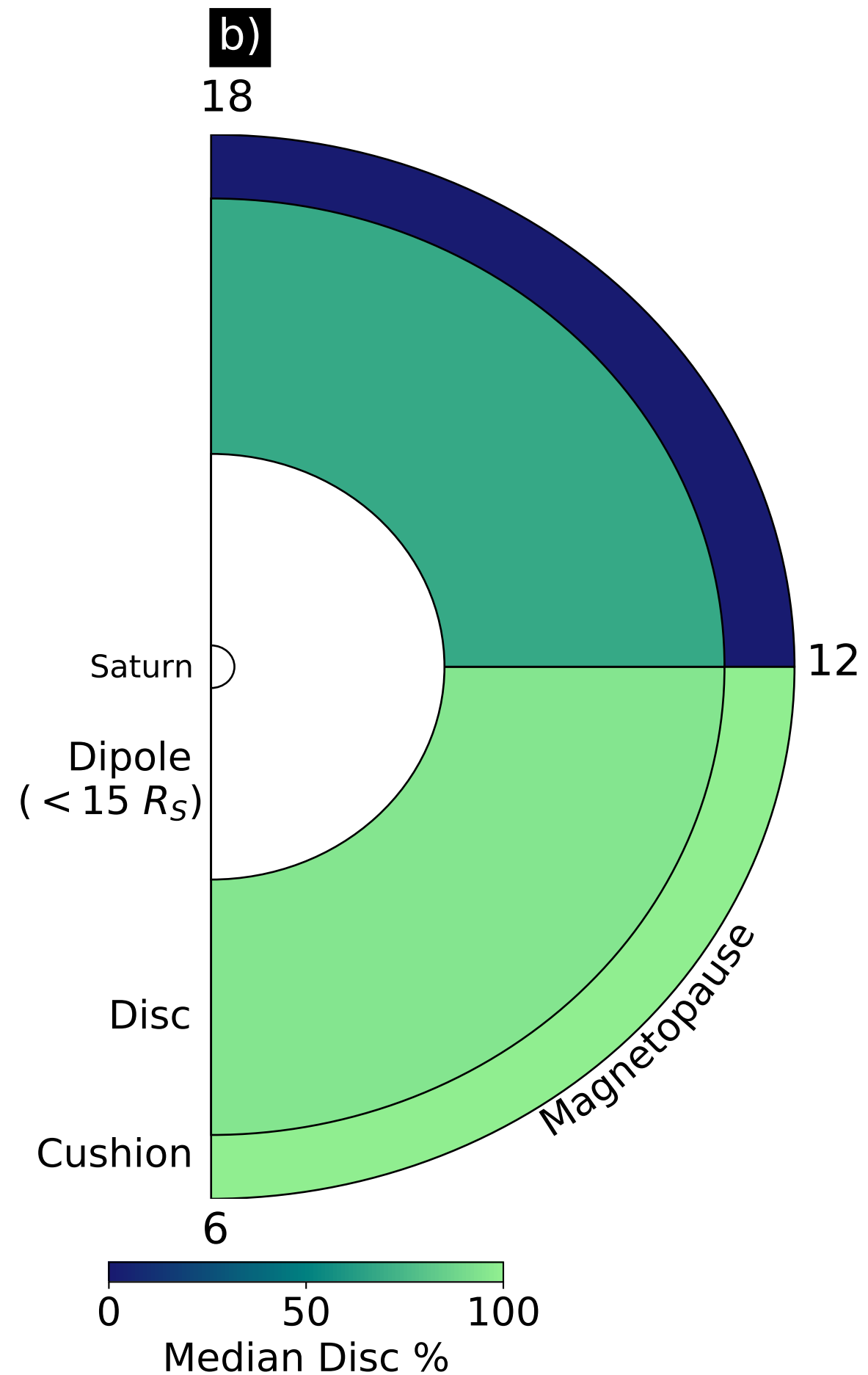
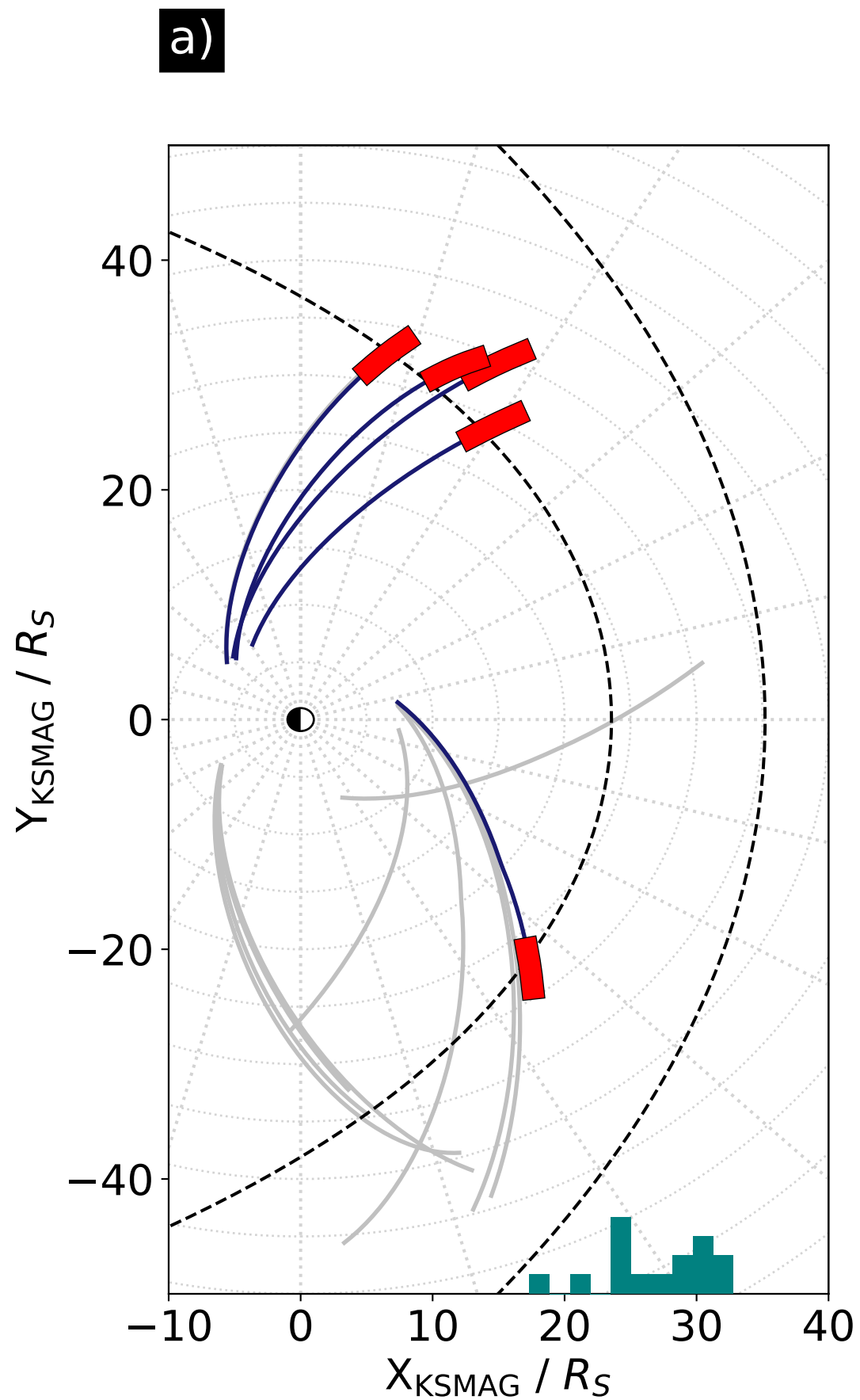


Figure 4.

